Bypass of a protein barrier by a replicative DNA helicase

Hasan Yardimci[1], Xindan Wang[2], Anna B. Loveland[1], Inger Tappin[3], David Z. Rudner[2], Jerard Hurwitz[3], Antoine M. van Oijen[4]* & Johannes C. Walter[1]*

Replicative DNA helicases generally unwind DNA as a single hexamer that encircles and translocates along one strand of the duplex while excluding the complementary strand (known as steric exclusion). By contrast, large T antigen, the replicative DNA helicase of the simian virus 40 (SV40), is reported to function as a pair of stacked hexamers that pumps double-stranded DNA through its central channel while laterally extruding single-stranded DNA. Here we use single-molecule and ensemble assays to show that large T antigen assembled on the SV40 origin unwinds DNA efficiently as a single hexamer that translocates on single-stranded DNA in the 3′-to-5′ direction. Unexpectedly, large T antigen unwinds DNA past a DNA–protein crosslink on the translocation strand, suggesting that the large T antigen ring can open to bypass bulky adducts. Together, our data underscore the profound conservation among replicative helicase mechanisms, and reveal a new level of plasticity in the interactions of replicative helicases with DNA damage.

An essential step in DNA replication is the unwinding of the double helix by a DNA helicase[1,2]. In general, these enzymes form a hexameric ring that encircles and translocates along one DNA strand in the 3′-to-5′ or 5′-to-3′ direction while excluding the other strand. This steric exclusion mechanism of DNA unwinding has been demonstrated for gp4 protein in phage T7 (ref. 3), DnaB in bacteria[4], and MCM2–7 in eukaryotes[5,6].

The mammalian DNA tumour virus SV40 encodes a multifunctional protein, large T antigen, which functions as a replicative helicase that cooperates with host cell replication factors to copy the SV40 genome. Although cell-free SV40 replication has served as a model for mammalian DNA replication for several decades[7], fundamental aspects of how large T antigen unwinds DNA remain controversial[8]. In particular, it is unclear whether large T antigen functions as an obligate double hexamer (Fig. 1A, a and b) or as a single hexamer (Fig. 1A, c and d). In support of the double-hexamer model, large T antigen caught in the act of unwinding displayed 'rabbit ear' structures with two single-stranded DNA (ssDNA) loops emanating from the double hexamer[9] (Fig. 1A, a and b). In addition, mutations in large T antigen that disrupt double-hexamer formation inhibit origin-dependent DNA unwinding[10,11]. Finally, purified large T antigen double hexamers exhibit higher unwinding activity than single hexamers on forked DNA substrates[12,13]. Another long-standing question is whether large T antigen unwinds DNA by means of steric exclusion (Fig. 1A, a and c) or a fundamentally different mechanism in which the translocating helicase encircles duplex DNA while extruding ssDNA from side channels (Fig. 1A, b and d). Large T antigen can translocate on ssDNA in the 3′-to-5′ direction when presented with a ssDNA template[14–16], and the closely related E1 helicase encircles ssDNA in its central channel[17], supporting the steric exclusion model. Consistent with the double-stranded DNA (dsDNA) translocation model, structural studies showed that the central channel of large T antigen can expand to accommodate dsDNA and that large T antigen has side channels large enough for extrusion of ssDNA[18,19].

Furthermore, several studies suggest that large T antigen assembled on the SV40 origin encircles dsDNA[20–22]. These results raise the possibility that large T antigen activated at an origin uses a dsDNA translocation mode. Inspired in part by large T antigen, both the double-hexamer and dsDNA translocation models were proposed for MCM2–7 (refs 23, 24), but recent evidence indicates that the native MCM2–7 complex unwinds DNA by steric exclusion and can function as a single hexamer[5,25].

Uncoupling of large T antigen double hexamers

The double-hexamer model suggests that DNA is pumped towards the interface between two large T antigen hexamers (Fig. 1A, a and b). Therefore, an extended DNA molecule that is attached to a surface at both ends should not be replicated efficiently owing to tension that accumulates at the ends of the DNA (Supplementary Fig. 1c). By contrast, if large T antigen can function as a single hexamer, a stretched DNA molecule should undergo extensive large-T-antigen-dependent replication (Supplementary Fig. 1d). To distinguish between the single- and double-hexamer models, we replicated λ DNA containing the SV40 origin (λori) that was attached at one or both ends to the surface of a microfluidic flow cell (Fig. 1B). We first examined replication of singly tethered λori DNA. After immobilizing DNA on the surface[26], large T antigen was drawn into the flow cell, allowing it to assemble on the origin (Fig. 1B). HeLa cell extract containing replication proteins[27,28] was then introduced to initiate replication, followed, after 20 min, by a second extract containing digoxigenin-modified dUTP (dig-dUTP) to pulse-label newly replicated DNA. After further incubation, dsDNA was stained with SYTOX Orange (SYTOX), and dig-dUTP-containing regions were labelled with fluorescein-conjugated anti-digoxigenin antibody (anti-dig). On 10–20% of the molecules, the SYTOX signal showed a high intensity tract (Fig. 1C, left, and Supplementary Fig. 2a) corresponding to a replication bubble. Furthermore, two anti-dig tracts were present at the ends of each replication bubble, consistent with bidirectionally

[1]Department of Biological Chemistry and Molecular Pharmacology, Harvard Medical School, Boston, Massachusetts 02115, USA. [2]Department of Microbiology and Immunobiology, Harvard Medical School, Boston, Massachusetts 02115, USA. [3]Program of Molecular Biology, Memorial Sloan–Kettering Cancer Center, New York, New York 10065, USA. [4]The Zernike Institute for Advanced Materials, University of Groningen, 9747 AG Groningen, The Netherlands.
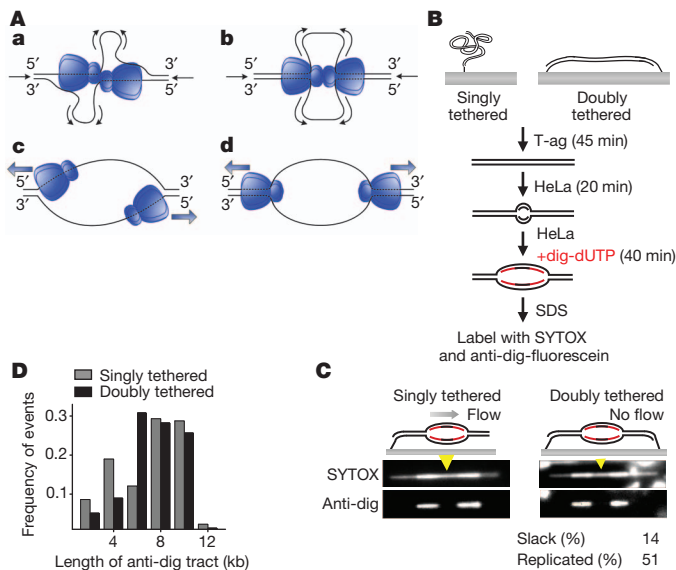*These authors contributed equally to this work.

Figure 1 | Large T antigen is not an obligate double hexamer during replication. **A**, Models for DNA unwinding by large T antigen (T-ag). See main text for details. **B**, Experimental procedure for replication of singly and doubly tethered λori DNA. **C**, SYTOX and anti-dig images of singly tethered (left) and doubly tethered (right) λori DNAs that underwent replication in HeLa cell extracts. Dig-dUTP-incorporated regions occasionally exhibited higher SYTOX intensity owing to nonspecific staining of an anti-dig antibody with SYTOX. Extent of slack and replication on the doubly tethered DNA are indicated. Yellow arrowheads, estimated position of the origin. **D**, Length of anti-dig tracts on singly tethered (grey) and doubly tethered (black) DNA molecules after a 40-min dig-dUTP pulse. To measure the fork rate, the tract length distribution was fit to a Gaussian and the resulting average tract length was divided by the duration of the dig-dUTP pulse (40 min).

growing bubbles (Fig. 1C, left, and Supplementary Fig. 2a). The gap between two anti-dig tracts always coincided with the expected location of the origin (Fig. 1C and Supplementary Fig. 2, yellow arrowheads), and replication bubbles were not observed on λ DNA lacking the SV40 origin (data not shown). The average fork rate measured from the anti-dig tract length was 188 ± 61 base pairs (bp) min^{-1} (mean $\pm$ s.d., $n = 174$, Fig. 1D) in agreement with previous reports[29,30]. Therefore, this single-molecule approach is well suited to study large-T-antigen-dependent replication.

We repeated the experiment on λori DNA that was stretched to 85–90% of its B-form contour length and tethered at both 3′ ends. If large T antigen functions as an obligate double hexamer, a doubly tethered DNA will not be replicated to a greater extent than the slack (10–15%) that is initially present in the molecule. In contrast to this prediction, we found that doubly tethered λori molecules contained replication bubbles comprising much more than 10–15% of the molecule (Fig. 1C, right, and Supplementary Fig. 2b, c), indicating that individual large T antigen hexamers function efficiently, similar to MCM2–7 (ref. 25). Importantly, the average fork rate on doubly tethered DNA (195 ± 75 bp min^{-1}, $n = 78$, Fig. 1D) was essentially the same as on singly tethered DNA, suggesting that any uncoupling of double hexamers does not impair fork progression. Finally, as expected from independently functioning replisomes, progression of sister forks showed no correlation on singly tethered ($R = 0.17$, $P = 0.11$, $n = 87$, Supplementary Fig. 2d) and doubly tethered ($R = -0.15$, $P = 0.35$, $n = 39$, Supplementary Fig. 2d) λori molecules.

To visualize the spatial separation of large T antigen double hexamers in real time, we examined large-T-antigen-mediated DNA unwinding on doubly tethered λori (Fig. 2a) using the ssDNA-binding replication protein A (RPA) fused to the green fluorescent protein (GFP)-like protein mKikGR (RPA^{mKikGR}). We detected bidirectionally growing linear tracts of RPA^{mKikGR} (Fig. 2b), demonstrating that large T antigen double
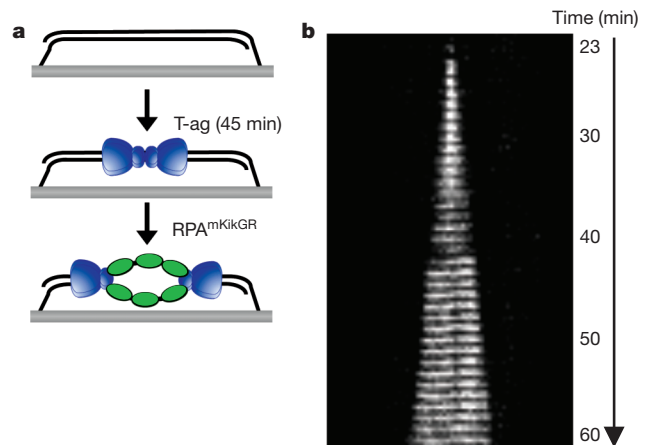

Figure 2 | Real-time visualization of sister fork uncoupling during unwinding of doubly tethered DNA. **a**, Large T antigen was drawn into a flow cell containing doubly tethered λori. After 45 min, RPA^{mKikGR} was introduced and mKikGR was imaged for 60 min. **b**, Kymograph of mKikGR fluorescence. Minutes denote time after introduction of RPA^{mKikGR}.

hexamers can uncouple after initiation. The average unwinding rate (215 ± 24 bp min^{-1} $\pm$ s.d., $n = 16$), determined through the growth rate of RPA^{mKikGR} tracts, was consistent with the unwinding rate of purified large T antigen[30] and our analysis of anti-dig tracts (Fig. 1D). The fact that DNA unwinding by large T antigen alone occurs at a similar rate as large-T-antigen-dependent replication indicates that large T antigen does not require coupling with a DNA polymerase to unwind DNA at optimal rates, unlike some prokaryotic helicases[31,32].

Large T antigen unwinds DNA by steric exclusion

We next examined whether large T antigen that initiates unwinding from the SV40 origin ultimately translocates on ssDNA or dsDNA. To this end, large T antigen was collided with biotin–streptavidin adducts, which large T antigen is known to disrupt[15]. We modified a 518-bp-long linear duplex DNA containing the SV40 origin with a site-specific biotin on the top or bottom strands (Fig. 3A, a). If large T antigen translocates on ssDNA in the 3′-to-5′ direction, the hexamer moving to the right from the origin should remove streptavidin from the bottom strand (SA^{bottom}) but not the top strand (SA^{top}) (Fig. 3A, b). By contrast, the dsDNA translocation model predicts that both SA^{bottom} and SA^{top} will be dislodged by large T antigen (Fig. 3A, c). We found that large T antigen displaced SA^{bottom} (Fig. 3B, lane 8, red arrowhead, and Supplementary Fig. 3) but not SA^{top} (Fig. 3B, lane 6, green arrowhead, and Supplementary Fig. 3), indicating that the bottom strand passes through the central chamber of large T antigen while the top strand is excluded (see Fig. 3C for quantification). We conclude that large T antigen that assembles on the origin DNA translocates on the leading strand template in the 3′-to-5′ direction.

To examine the translocation mechanism of large T antigen during DNA replication, we attached a quantum dot (Qdot) by a digoxigenin–anti-dig interaction to either the leading (Qdot^{lead}) or lagging (Qdot^{lag}) strand templates to the left of the origin on λori (Fig. 3D, cartoons). As in the experiment above, the 3′-to-5′ ssDNA translocation model predicts the specific removal of Qdot^{lead}, whereas the dsDNA translocation model predicts the removal of both Qdot^{lead} and Qdot^{lag}. Because most Qdots dissociated from λori independently of replication (Supplementary Fig. 4 and data not shown), we could not compare replicated molecules that retained and lost Qdots, respectively, to evaluate Qdot removal by the replisome. Given that large T antigen can displace streptavidin (Fig. 3B), most events in which the edge of an anti-dig tract coincided with a Qdot (Fig. 3D and Supplementary Fig. 4f) are likely to represent spontaneous fork stalling independently of the Qdot (see Supplementary Fig. 2 for examples of spontaneous fork stalling). Because the likelihood of such an
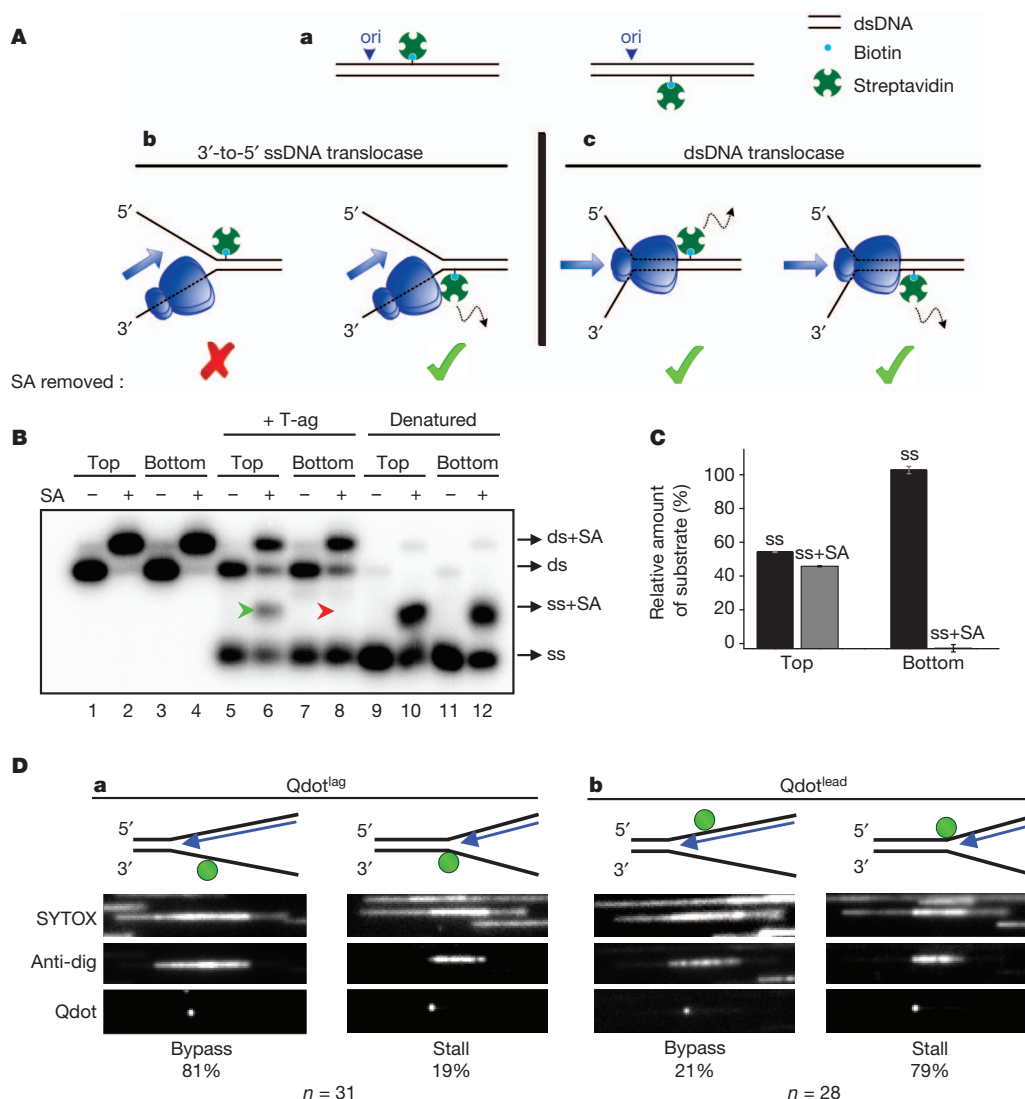
Figure 3 | Large T antigen translocates on ssDNA in the 3′-to-5′ direction.
A, a, Cartoon of 518-bp-long 5′-labelled (red stars) DNA templates used for streptavidin displacement assays. **A, b, c,** Predictions of 3′-to-5′ ssDNA translocation (**b**) and dsDNA translocation (**c**) models. **B,** DNAs biotinylated on the top or bottom strands (as in **A, a**) undergo complete mobility shift after streptavidin (SA) addition, indicating that all DNA molecules are modified with biotin (lanes 2, 4). DNA was pre-incubated with buffer (lanes 5, 7) or streptavidin (lanes 6, 8), and unwinding was initiated with large T antigen and RPA (lanes 5–8). Excess biotin saturated any displaced streptavidin. To assess the migration of ssDNA with or without streptavidin, DNA was heat denatured, rapidly cooled down and mixed with buffer (lanes 9, 11) or streptavidin (lanes 10, 12). Because both strands are radiolabelled, streptavidin association with one strand shifts only half of the signal (lanes 10, 12). ds, dsDNA; ss, ssDNA. **C,** Quantification of
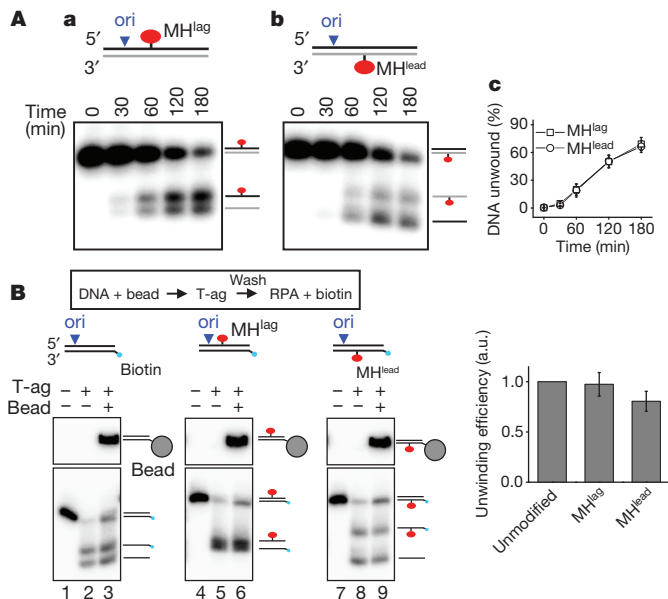
ssDNA with (grey) and without (black) streptavidin from lanes 6 and 8 of **B**. Error bars indicate s.d. for three independent experiments. Some spontaneous dissociation of streptavidin occurred in the presence of free biotin (**B**, lanes 6 and 8, ds). The extent of large-T-antigen-independent streptavidin dissociation was determined using the relative amounts of dsDNA that lost (ds) and retained SA (ds+SA). This fraction was then used to measure the amount of ssDNA that lost and retained streptavidin, respectively, if no spontaneous streptavidin dissociation had occurred. **D, a, b,** SYTOX, anti-dig and Qdot images of representative molecules after fork collision with Qdot[lag] (**a**) or Qdot[lead] (**b**) in HeLa cell extracts (performed as in Fig. 1B). Because dig-dUTP was continuously present during the replication reaction, replication bubbles were fully labelled with anti-dig. The percentage of molecules exhibiting fork bypass and stalling events is indicated (see also Supplementary Fig. 4).

event is the same for Qdot[lead] and Qdot[lag], we determined the ratio of molecules showing fork bypass through a Qdot (Supplementary Fig. 4e) to those exhibiting stalling at the Qdot (Supplementary Fig. 4f) to obtain a relative probability of Qdot removal by the replisome. Importantly, 81% of the molecules exhibited fork bypass through Qdot[lag] (Fig. 3D, a) whereas only 21% bypass was observed through Qdot[lead] (Fig. 3D, b), suggesting that Qdot[lead] is more prone to displacement by the replisome. This result suggests that large T antigen also functions as a 3′-to-5′ ssDNA translocase during DNA replication.

Large T antigen can bypass a bulky protein adduct

Given that large T antigen encircles and translocates on the leading strand template, our observation that a considerable number of

anti-dig tracts bypassed Qdot[lead] was unexpected (Fig. 3D, b, left panel). Bypass through Qdot[lead] indicates that large T antigen or other helicases in the extract can circumvent a bulky adduct on the leading strand template. To test this idea further, we covalently conjugated HpaII methyltransferase (M.HpaII) to the lagging (MH[lag]) or leading (MH[lead]) strand templates of a 518-bp-long linear DNA substrate containing the SV40 origin (Supplementary Fig. 5a). Notably, large T antigen unwound DNA containing MH[lag] and MH[lead] equally well (Fig. 4A). MH[lead] was not removed from DNA by large T antigen during unwinding, as seen by the presence of ssDNA conjugated to M.HpaII (Fig. 4A, b). Uneven labelling of the two strands resulted in the intensity difference of ssDNA with and without M.HpaII (Supplementary Fig. 5b).

Figure 4 | Large T antigen can bypass a covalent protein barrier on the translocation strand. A, a, b, Large-T-antigen-dependent unwinding of DNA containing MH^lag (**a**) or MH^lead (**b**). The species corresponding to each band are depicted. Heat denaturation caused electrophoretic smearing of M.HpaII-conjugated DNA and therefore was not used for assessment of ssDNA migration (data not shown). **A, c,** Quantification of unwinding in **a** and **b. B,** Left, unwinding of unmodified (lane 3), MH^lag-modified (lane 6), and MH^lead-modified (lane 9) DNA by pre-assembled large T antigen (see text for details). The first two lanes in all samples correspond to 10% of input DNA without bead conjugation in the absence (lanes 1, 4, 7) and presence (lanes 2, 5, 8) of large-T-antigen-mediated unwinding. Right, quantification of unwound DNA by pre-assembled large T antigen (lanes 3, 6, 9). Amount of unwinding was normalized to that of unmodified DNA. a.u., arbitrary units. Error bars indicate s.d. for three independent experiments.

We next addressed whether the same large T antigen that initially collides with MH^lead bypasses the protein adduct, or whether a new large T antigen hexamer from solution assembles downstream of the protein adduct. To this end, DNA was immobilized on magnetic beads, incubated with large T antigen to assemble the helicase at the origin, washed to remove free large T antigen, and finally mixed with RPA to initiate unwinding. We confirmed that during this sequence, unwinding initiated from the origin and that most unwinding was carried out by pre-assembled large T antigen (Supplementary Fig. 6). Importantly, large T antigen pre-assembled on the origin was sufficient to unwind the template containing MH^lead (Fig. 4B, left, lane 9), and unwinding efficiency was only moderately reduced relative to MH^lag (Fig. 4B, right). Thus, the vast majority of large T antigen molecules are able to bypass a bulky adduct on the translocation strand.
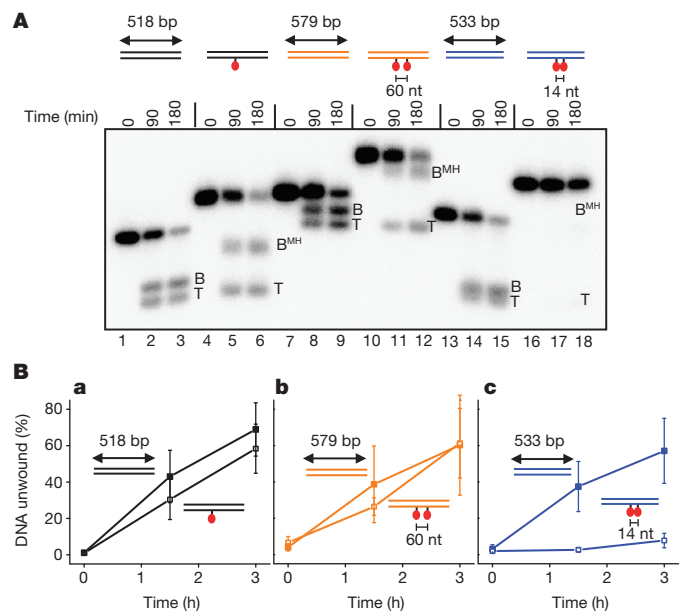
Large T antigen collision with two protein barriers

Our results suggest that after collision with a protein adduct, the large T antigen ring either opens to allow bypass (Supplementary Fig. 7a, ii) or denatures the protein adduct and threads the unfolded polypeptide chain through the helicase central channel (Supplementary Fig. 7a, iii). Because M.HpaII interacts with DNA by an internal amino acid[33], the latter model would require large T antigen to accommodate two polypeptide chains and ssDNA in its central channel (Supplementary Fig. 7a, iii), which seems unlikely. To rule out the denaturation model, we repeated the experiment with a DNA template containing two protein adducts spaced 60 nucleotides (~200 Å) apart along the duplex (Supplementary Fig. 7b, i). In this way, unwinding the DNA by M.HpaII denaturation would require four polypeptide chains and the translocation strand to be threaded through the central channel of large T antigen (Supplementary Fig. 7b, ii), which is incompatible

with known large T antigen structures[18,19]. Notably, large T antigen unwound the template with two adducts as efficiently as the unadducted template (Fig. 5A, compare lanes 9 and 12, and 5B, b, for quantification), suggesting that bypass must occur by transient opening of the large T antigen ring. We found that two M.HpaII adducts spaced 14 nucleotides apart severely inhibited unwinding by large T antigen (Fig. 5A, lane 18, and 5B, c). Because the longitudinal axis of large T antigen (~120 Å) is now greater than the inter-adduct distance (~50 Å), this result indicates that to perform effective bypass of the second obstruction, the large T antigen ring must re-close after the first adduct has traversed the entire channel (Supplementary Fig. 7b, iii and iv). Together, the data suggest that the large T antigen ring transiently opens to bypass protein–DNA crosslinks.

Discussion

Here we present single-molecule and ensemble experiments that determine the molecular mechanism by which large T antigen unwinds DNA at the replication fork. In contrast with the prominent double-hexamer model[23], we demonstrate that the large T antigen double hexamers that form at the origin of replication can physically separate and function independently when the DNA template is placed under tension. Together with previous results[10,11], our data suggest that interactions between hexamers are required for initiation but dispensable during elongation. The coupling between two hexamers that led to the observation of rabbit ear structures[9] may be due to direct interactions between hexamers or facilitated by other factors[34]. Whether such double hexamers are normally retained during replication elongation in the complex environment of the cell is difficult to assess. Importantly, the ability of hexamers to function independently is advantageous because it allows replication to go to completion even if one replisome stalls or collapses. Notably, we found that large T antigen that initiates unwinding from the origin ultimately surrounds ssDNA and moves in the 3′-to-5′ direction, as proposed for the related E1 helicase[17]. Taken together, our results

Figure 5 | Bypass of tandem protein adducts by large T antigen depends on the inter-adduct distance. A, Unwinding of DNA containing, none, one or two M.HpaII adducts on the translocation strand by large T antigen. The three templates (colour-coded differentially) had slightly different lengths because each template contained 240 bp before the first protein adduct and 277 bp after the last protein adduct but different amounts of DNA between the adducts. DNAs were internally labelled with [α^32P]-dATP. B, bottom strand; B^MH, bottom strand modified with M.HpaII; nt, nucleotide; T, top strand. **B,** Quantification of unwinding from three independent experiments as in **A**. Error bars indicate s.d.

emphasize that replicative helicases in different organisms use a common mechanism to unwind DNA.

Our results also show that large T antigen is able to bypass a protein crosslinked to the translocation strand, and they favour a model in which the bypass occurs by opening of the hexamer. This unprecedented flexibility of large T antigen may allow the SV40 replisome to bypass natural impediments including tightly bound proteins on DNA such as transcription complexes or covalently trapped proteins[35,36]. If large T antigen initially assembles around dsDNA at the origin[21,22], the ability of the large T antigen ring to open on DNA may also facilitate the exclusion of one strand from the central channel during replication initiation as proposed[37]. In the future, it will be important to confirm by more direct means that the large T antigen ring opens while bypassing a bulky adduct. Furthermore, determining whether other replicative helicases exploit similar plasticity to bypass replication barriers can guide our understanding of how these enzymes interact with DNA damage.

METHODS SUMMARY

For single-molecule experiments, λori DNA was annealed to 3′-biotin-modified oligonucleotides at its ssDNA end and attached to the streptavidin-functionalized surface of a microfluidic flow cell. Large T antigen and HeLa cell extracts were diluted in large T antigen binding (TAB) buffer containing 30 mM Hepes, pH 7.5, 7 mM MgCl$_2$, 0.5 mM dithiothreitol and 50 μg ml^{-1} BSA, and introduced into the flow cell. Total internal reflection fluorescence imaging was performed on a custom-built setup. Ensemble DNA unwinding assays were performed on radio-labelled PCR fragments in TAB buffer supplemented with large T antigen and RPA.

Full Methods and any associated references are available in the online version of the paper.

1. Patel, S. S. & Picha, K. M. Structure and function of hexameric helicases. *Annu. Rev. Biochem.* **69,** 651–697 (2000).
2. Enemark, E. J. & Joshua-Tor, L. On helicases and other motor proteins. *Curr. Opin. Struct. Biol.* **18,** 243–257 (2008).
3. Egelman, E. H., Yu, X., Wild, R., Hingorani, M. M. & Patel, S. S. Bacteriophage T7 helicase/primase proteins form rings around single-stranded DNA that suggest a general structure for hexameric helicases. *Proc. Natl Acad. Sci. USA* **92,** 3869–3873 (1995).
4. Kaplan, D. L. & O'Donnell, M. Twin DNA pumps of a hexameric helicase provide power to simultaneously melt two duplexes. *Mol. Cell* **15,** 453–465 (2004).
5. Fu, Y. V. *et al.* Selective bypass of a lagging strand roadblock by the eukaryotic replicative DNA helicase. *Cell* **146,** 931–941 (2011).
6. Kaplan, D. L., Davey, M. J. & O'Donnell, M. Mcm4,6,7 uses a "pump in ring" mechanism to unwind DNA by steric exclusion and actively translocate along a duplex. *J. Biol. Chem.* **278,** 49171–49182 (2003).
7. Fanning, E. & Zhao, K. SV40 DNA replication: from the A gene to a nanomachine. *Virology* **384,** 352–359 (2009).
8. Fanning, E., Zhao, X. & Jiang, X. in *DNA Tumor Viruses* (eds Damania, B. & Pipas, J. M.) 1–24 (Springer US, 2009).
9. Wessel, R., Schweizer, J. & Stahl, H. Simian virus 40 T-antigen DNA helicase is a hexamer which forms a binary complex during bidirectional unwinding from the viral origin of DNA replication. *J. Virol.* **66,** 804–815 (1992).
10. Weisshart, K. *et al.* Two regions of simian virus 40 large T antigen determine cooperativity of double-hexamer assembly on the viral origin of DNA replication and promote hexamer interactions during bidirectional origin DNA unwinding. *J. Virol.* **73,** 2201–2211 (1999).
11. Barbaro, B. A., Sreekumar, K. R., Winters, D. R., Prack, A. E. & Bullock, P. A. Phosphorylation of simian virus 40 large T antigen on Thr 124 selectively promotes double-hexamer formation on subfragments of the viral core origin. *J. Virol.* **74,** 8601–8613 (2000).
12. Smelkova, N. V. & Borowiec, J. A. Dimerization of simian virus 40 T-antigen hexamers activates T-antigen DNA helicase activity. *J. Virol.* **71,** 8766–8773 (1997).
13. Alexandrov, A. I., Botchan, M. R. & Cozzarelli, N. R. Characterization of simian virus 40 T-antigen double hexamers bound to a replication fork. *J. Biol. Chem.* **277,** 44886–44897 (2002).
14. SenGupta, D. J. & Borowiec, J. A. Strand-specific recognition of a synthetic DNA replication fork by the SV40 large tumor antigen. *Science* **256,** 1656–1661 (1992).
15. Morris, P. D. *et al.* Hepatitis C virus NS3 and simian virus 40 large T antigen helicases displace streptavidin from 5′-biotinylated oligonucleotides but not from 3′-biotinylated oligonucleotides: evidence for directional bias in translocation on single-stranded DNA. *Biochemistry* **41,** 2372–2378 (2002).
16. Goetz, G. S., Dean, F. B., Hurwitz, J. & Matson, S. W. The unwinding of duplex regions in DNA by the simian virus 40 large tumor antigen-associated DNA helicase activity. *J. Biol. Chem.* **263,** 383–392 (1988).
17. Enemark, E. J. & Joshua-Tor, L. Mechanism of DNA translocation in a replicative hexameric helicase. *Nature* **442,** 270–275 (2006).
18. Li, D. *et al.* Structure of the replicative helicase of the oncoprotein SV40 large tumour antigen. *Nature* **423,** 512–518 (2003).
19. Gai, D., Zhao, R., Li, D., Finkielstein, C. V. & Chen, X. S. Mechanisms of conformational change for a replicative hexameric helicase of SV40 large tumor antigen. *Cell* **119,** 47–60 (2004).
20. Gomez-Lorenzo, M. G. *et al.* Large large T antigen on the simian virus 40 origin of replication: a 3D snapshot prior to DNA replication. *EMBO J.* **22,** 6205–6213 (2003).
21. Cuesta, I. *et al.* Conformational rearrangements of SV40 large large T antigen during early replication events. *J. Mol. Biol.* **397,** 1276–1286 (2010).
22. Borowiec, J. A. & Hurwitz, J. ATP stimulates the binding of simian virus 40 (SV40) large tumor antigen to the SV40 origin of replication. *Proc. Natl Acad. Sci. USA* **85,** 64–68 (1988).
23. Sclafani, R. A., Fletcher, R. J. & Chen, X. S. Two heads are better than one: regulation of DNA replication by hexameric helicases. *Genes Dev.* **18,** 2039–2045 (2004).
24. Takahashi, T. S., Wigley, D. B. & Walter, J. C. Pumps, paradoxes and ploughshares: mechanism of the MCM2–7 DNA helicase. *Trends Biochem. Sci.* **30,** 437–444 (2005).
25. Yardimci, H., Loveland, A. B., Habuchi, S., van Oijen, A. M. & Walter, J. C. Uncoupling of sister replisomes during eukaryotic DNA replication. *Mol. Cell* **40,** 834–840 (2010).
26. Yardimci, H., Loveland, A. B., van Oijen, A. M. & Walter, J. C. Single-molecule analysis of DNA replication in *Xenopus* egg extracts. *Methods* **57,** 179–186 (2012).
27. Stillman, B. W. & Gluzman, Y. Replication and supercoiling of simian virus 40 DNA in cell extracts from human cells. *Mol. Cell. Biol.* **5,** 2051–2060 (1985).
28. Wobbe, C. R., Dean, F., Weissbach, L. & Hurwitz, J. *In vitro* replication of duplex circular DNA containing the simian virus 40 DNA origin site. *Proc. Natl Acad. Sci. USA* **82,** 5710–5714 (1985).
29. Bullock, P. A., Seo, Y. S. & Hurwitz, J. Initiation of simian virus 40 DNA synthesis *in vitro. Mol. Cell. Biol.* **11,** 2350–2361 (1991).
30. Murakami, Y. & Hurwitz, J. Functional interactions between SV40 large T antigen and other replication proteins at the replication fork. *J. Biol. Chem.* **268,** 11008–11017 (1993).
31. Kim, S., Dallmann, H. G., McHenry, C. S. & Marians, K. J. Coupling of a replicative polymerase and helicase: a τ-DnaB interaction mediates rapid replication fork movement. *Cell* **84,** 643–650 (1996).
32. Stano, N. M. *et al.* DNA synthesis provides the driving force to accelerate DNA unwinding by a helicase. *Nature* **435,** 370–373 (2005).
33. Chen, L. *et al.* Direct identification of the active-site nucleophile in a DNA (cytosine-5)-methyltransferase. *Biochemistry* **30,** 11018–11025 (1991).
34. Seinsoth, S., Uhlmann-Schiffler, H. & Stahl, H. Bidirectional DNA unwinding by a ternary complex of large T antigen, nucleolin and topoisomerase I. *EMBO Rep.* **4,** 263–268 (2003).
35. Barker, S., Weinfeld, M. & Murray, D. DNA-protein crosslinks: their induction, repair, and biological consequences. *Mutat. Res.* **589,** 111–135 (2005).
36. Anand, R. P. *et al.* Overcoming natural replication barriers: differential helicase requirements. *Nucleic Acids Res.* **40,** 1091–1105 (2011).
37. Wu, C., Roy, R. & Simmons, D. T. Role of single-stranded DNA binding activity of large T antigen in simian virus 40 DNA replication. *J. Virol.* **75,** 2839–2847 (2001).

Author Contributions H.Y., A.M.v.O. and J.C.W. designed the experiments. H.Y. performed the experiments. X.W. and D.Z.R. supervised and assisted H.Y. for construction of λori DNA. A.B.L. made fluorescently tagged RPA. I.T. and J.H. provided RPA and large T antigen. H.Y., A.M.v.O. and J.C.W. interpreted the data and wrote the paper. X.W. and A.B.L. contributed equally.

Author Information Reprints and permissions information is available at www.nature.com/reprints. The authors declare no competing financial interests. Readers are welcome to comment on the online version of the paper. Correspondence and requests for materials should be addressed to A.M.V. (a.m.van_oijen@rug.nl) or J.C.W. (johannes_walter@hms.harvard.edu).

METHODS

Protein expression and purification. SV40 large large T antigen[38] and RPA[39] were expressed and purified as described. Fluorescently tagged RPA was made by cloning mKikGR and a histidine-tag onto the amino terminus of the RPA70 subunit. RPA^{mKikGR} was purified by Ni-NTA chromatography.

Preparation of λori. To construct the λ DNA with the SV40 origin (λori), we first carried out a series of cloning steps to generate a plasmid that contains a 4.7-kb DNA fragment including the 233 bp SV40 origin region from pUC.HSO[40] at one end, a 22-bp sequence (5′-CCTCAGCATAGATGTCCTCAGC-3′) for Qdot attachment at the other end, and a 4.5-kb DNA spacer in between, which contains a tetracycline-resistance gene, an ampicillin-resistance gene and part of a *Bacillus subtilis* non-essential gene, *yrvN*. This fragment was PCR-amplified using primers flanking with 40-bp sequences homologous to the λ genome (5′-ACAG CCCGCCGGAACCGGTGGGCTTTTTTGTGGGGTGAAT-3′ and 5′-CCTGC GGCATATCACAAAACGATTACTCCATAACAGGGACA-3′), and electroporated into a lysogen MC4100 (λ CI857 Sam7)[41] to replace two non-essential genes (*stf* and *tfa*) in the prophage using a recombineering method[42]. The modified λ DNA was purified from the lysogen by Lofstrand Labs Limited.

Labelling λori with Qdot. λori contains a 22-bp sequence (5′-CCTC AGCATAGATGTCCTCAGC-3′) approximately 4 kb away from the SV40 origin. This sequence has two sequential sites (5′-CCTCAGC-3′) that are recognized by nicking enzymes Nt.BbvCI and Nb.BbvCI. We used Nt.BbvCI or Nb.BbvCI, respectively, to modify either the top or bottom strands of λori with a digoxigenin at a single base according to a previously established protocol[43,44]. To place a digoxigenin in the top strand, λori was treated with Nt.BbvCI, mixed with 100-fold molar excess of oligonucleotide (5′-TCAGCAT^{dig}AGATGTCC-3′, Biosynthesis) containing a digoxigenin at T^{dig}, heated to 60 °C, and slowly cooled down to room temperature. This procedure leads to melting of a 15-nucleotide region between the two Nt.BbvCI sites, which is then replaced by the digoxigenin-modified oligonucleotide. The modified oligonucleotide was then ligated to λori using T4 DNA Ligase (NEB). The same procedure was performed to modify the bottom strand of λori with digoxigenin except that DNA was nicked with Nb.BbvCI and annealed and ligated to 5′-TGAGGACAT^{dig}CTATGC-3′. Attachment of anti-dig-conjugated Qdot605 (Invitrogen) to surface-immobilized λori was performed as described[5].

Preparation of DNA constructs. To produce biotin-modified linear DNA for use in ensemble unwinding assays, we cloned an insert (5′-CCTCAGCAGATA TCACCTCAGC-3′) between the EcoRI and NdeI sites of the pUC.HSO vector[40] that places the insert approximately 150 nucleotides away from the SV40 origin. A 518-bp fragment within the resulting vector was PCR-amplified using the following oligonucleotides: forward: 5′-CCTCCAAAAAGGCTCCTCACTA-3′, reverse: 5′-GTGCCACCTGACGTCTAAGAAACC-3′.

The length of the DNA substrate was chosen such that dsDNA (Fig. 3B, lanes 1 and 3), dsDNA bound to streptavidin (Fig. 3B, lanes 2 and 4), ssDNA (Fig. 3B, lanes 9 and 11), and ssDNA bound to streptavidin (Fig. 3B, lanes 10 and 12) ran at discrete positions on a 3% agarose gel. The PCR fragment contains the origin near one end and the 22-bp insert close to the centre (Fig. 3A). We first inserted an amine residue on the top or bottom strands using the same template exchange strategy as before. DNA was either nicked with Nt.BbvCI and annealed/ligated to 5′-TGAGGTGAT^{amn}ATCTGC-3′ (to modify the top strand), or nicked with Nb.BbvCI and annealed/ligated to 5′-TCAGCAGAT^{amn}ATCACC-3′ (to modify the bottom strand). Modified oligonucleotides were purchased from IDT that contained a C6-amine at T^{amn}. To attach biotin to the amine-modified thymidine residue, amine-modified DNA (400 ng) was mixed with NHS-PEG4-biotin (2.5 μl of 100 μM dissolved in dimethylsulphoxide, Pierce) in PBS buffer (25 μl final volume), and incubated overnight at room temperature. Excess NHS-PEG4-amine was removed by running DNA on a 1.5% agarose gel and subsequent gel extraction of DNA. This protocol generally resulted in half of the DNA molecules being modified with biotin at the specific site. To purify biotinylated DNA selectively, DNA was mixed with streptavidin (0.6 mg ml^{-1} final), incubated for at least 2 h and separated on a 1.5% agarose gel. We then excised the band corresponding to the streptavidin-bound DNA that ran slower than free DNA. Purification of DNA from agarose gel was performed using a QIAquick gel extraction kit (Qiagen) unless stated otherwise. We note that streptavidin dissociated from biotin on DNA during the gel purification process, possibly owing to the denaturation of streptavidin by the ethanol wash of the spin column.

To conjugate M.HpaII covalently to DNA, we first cloned 5′- CCTCAGCA T**CCGG**TACCTCAGC-3′ between the EcoRI and NdeI sites of the pUC.HSO (in which bold denotes the sequence recognized by M.HpaII). We then used the same primers as before to make a 518-bp PCR fragment containing the origin and the insert. The same nicking strategy described above was used to insert a 5-fluoro-2′-deoxycytidine (C^{fluo})-modified oligonucleotide to either the top or bottom strands for subsequent covalent attachment of M.HpaII to DNA[33,45]. The

PCR fragment was either nicked with Nt.BbvCI and annealed/ligated to 5′-TCAGCATCC^{fluo}GGTACC-3′ (to modify the top strand), or nicked with Nb.BbvCI and annealed/ligated to 5′-TGAGGTACC^{fluo}GGATGC-3′ (to modify the bottom strand). Custom-synthesized 5-fluoro-modified oligonucleotides were purchased from Biosynthesis. Modified DNA was gel-purified as described above and mixed with M.HpaII (1,000 U ml^{-1} final, NEB) in HpaII methylase reaction buffer (50 mM Tris-HCl, pH 7.5, 5 mM 2-mercaptoethanol, 10 mM EDTA) supplemented with 100 μM *S*-adenosylmethionine. After 6–9 h of incubation at 37 °C, DNA was separated on a 1.5% agarose gel and the slow migrating band corresponding to M.HpaII-conjugated DNA was excised. To prevent denaturation of M.HpaII, DNA was purified by electroelution. In brief, the gel fragment containing M.HpaII-bound DNA was placed in a dialysis tube (3.5 kilodalton cut-off) filled with TBE buffer, and electrophoresis was used to run the DNA off the gel into the dialysis tube. The gel fragment was then removed from the tube, and DNA was dialysed against 10 mM Tris, pH 8, and concentrated using a spin concentrator (Ultrafree Biomax-10K, ThermoFisher Scientific).

To generate DNA constructs containing two M.HpaII adducts, we first cloned two inserts of the same sequence (5′-CCTCAGCAT**CCGG**TACCTCAGC-3′; in which bold denotes the sequence recognized by M.HpaII) into pUC.HSO that were separated by reported lengths. After making a PCR product of the desired length, the same protocol as above was used for insertion of 5-fluoro-2′-deoxycytidine-modified oligonucleotide and subsequent M.HpaII conjugation.

Single-molecule DNA replication and unwinding assays. A microfluidic flow cell with a streptavidin-functionalized bottom surface was prepared as described[46]. Similar to the wild-type λ DNA, λori contains 12-nucleotide ssDNA at both ends. λori was biotinylated and singly or doubly tethered to the surface using biotin-modified oligonucleotides complementary to these ends as described[26]. For large-T-antigen-dependent replication of λori in HeLa cell extracts, the flow cell containing surface-immobilized λori molecules was placed on a heat block (VWR) set to 37 °C. The flow cell was flushed with 50 μl large T antigen binding (TAB) buffer containing 30 mM Hepes, pH 7.5, 7 mM MgCl$_2$, 0.5 mM dithiothreitol (DTT) and 50 μg ml^{-1} BSA. Large T antigen (10 μg ml^{-1}) was introduced into the flow cell in TAB buffer supplemented with an ATP regeneration mixture (4 mM ATP, 50 mM phosphocreatine and 10 ng μl^{-1} creatine phosphokinase), and 5 ng μl^{-1} competitor DNA (pUC19) for origin-specific assembly of large T antigen[16], and incubated for the indicated times.

For large-T-antigen-dependent replication, a replication mixture was prepared by diluting 15 μl HeLa cell extract (Chimerx) twofold in buffer containing 30 mM Hepes, pH 7.5, 7 mM MgCl$_2$, 0.5 mM DTT, 50 μg ml^{-1} BSA, 4 mM ATP, 50 mM phosphocreatine, 10 ng μl^{-1} creatine phosphokinase, 0.1 mM each of dATP, dGTP, dTTP and dCTP, and 50 μM each of GTP, TTP and CTP (all concentrations final). The replication mixture was drawn into the flow cell and incubated for the indicated times. To confirm bidirectional replication, a second replication mixture containing 1.7 μM dig-dUTP was drawn into the flow cell and further incubated. Competitor DNA (pUC19; 5 ng μl^{-1}) was included to suppress nonspecific interaction of proteins in the extract with λori that interferes with fork progression (data not shown). To stop the reaction, the flow cell was washed with buffer containing 20 mM Tris, pH 7.5, 50 mM NaCl, 12 mM EDTA and 0.1% SDS.

To visualize unwinding of λori by large T antigen in real time, large T antigen was first assembled on doubly tethered λori as described above. RPA^{mKikGR} (15 nM) was then drawn into the flow cell in TAB supplemented with the ATP regeneration mixture. The flow cell was heated to 37 °C on a microscope stage with an objective heater (Bioptechs) during large T antigen assembly and subsequent unwinding reactions. Imaging of RPA^{mKikGR} is described below.

Ensemble DNA unwinding assays. PCR fragments were labelled either internally with [α^{32}P]-dATP (Perkin Elmer) during the PCR reaction, or at their 5′ ends using T4 polynucleotide kinase (NEB) and [γ^{32}P]-ATP (Perkin Elmer). Unwinding reactions were performed with 0.3–0.5 ng μl^{-1} labelled DNA, 10 μg ml^{-1} large T antigen, 40 μg ml^{-1} RPA and the ATP regeneration mixture in TAB and incubated for the indicated amount of time at 37 °C. Unlabelled competitor DNA (FspI linearized pUC19; 5 ng μl^{-1}) was included in unwinding reactions to ensure origin-specific unwinding. The reaction was stopped with 0.5% SDS and 20 mM EDTA, DNA was separated on a 3% agarose gel, and visualized using a phosphorimager. Quantification of band intensities was carried out using Quantity One software.

To prepare 5′-biotin-modified DNA for bead-immobilization, one of the primers used in the PCR reaction contained biotin at the 5′ end. Fifteen nanograms of DNA was mixed with streptavidin-coated magnetic beads (Invitrogen) in 10 mM Tris supplemented with 0.2 mg ml^{-1} BSA. Beads were washed twice using a magnet, resuspended in TAB buffer containing the ATP regeneration mixture and 20 μg ml^{-1} large T antigen, and incubated for 2.5 h at 37 °C rotating on a rotisserie. Beads were washed twice with TAB buffer containing 0.6 mM ATP,

resuspended in TAB buffer supplemented with the ATP regeneration mixture, $40\ \mu g\ ml^{-1}$ RPA, 50 μM biotin, 15 ng cold DNA containing the origin, and incubated for 30 min at 37 °C before stopping the reaction.

Single-molecule imaging. Total internal reflection fluorescence imaging was carried out on an inverted microscope (Olympus IX-71) using a ×60 oil objective (PlanApo, numerical aperture = 1.45, Olympus). SYTOX and fluorescein-anti-dig images on surface-immobilized DNA after replication in HeLa extracts were recorded as described[26]. Live monitoring of RPA[mKikGR] was performed by capturing an image every minute using 488-nm laser light.

38. Eki, T., Matsumoto, T., Murakami, Y. & Hurwitz, J. The replication of DNA containing the simian virus 40 origin by the monopolymerase and dipolymerase systems. *J. Biol. Chem.* **267,** 7284–7294 (1992).

39. Ishimi, Y., Claude, A., Bullock, P. & Hurwitz, J. Complete enzymatic synthesis of DNA containing the SV40 origin of replication. *J. Biol. Chem.* **263,** 19723–19733 (1988).

40. Wold, M. S., Li, J. J. & Kelly, T. J. Initiation of simian virus 40 DNA replication *in vitro*: large-tumor-antigen- and origin-dependent unwinding of the template. *Proc. Natl Acad. Sci. USA* **84,** 3643–3647 (1987).

41. Wang, I.-N. Lysis timing and bacteriophage fitness. *Genetics* **172,** 17–26 (2005).

42. Thomason, L. C., Oppenheim, A. B. & Court, D. L. Modifying bacteriophage lambda with recombineering. *Methods Mol Biol.* **501,** 239–251 (2009).

43. Kuhn, H. & Frank-Kamenetskii, M. D. Labeling of unique sequences in double-stranded DNA at sites of vicinal nicks generated by nicking endonucleases. *Nucleic Acids Res.* **36,** e40 (2008).

44. Loparo, J. J., Kulczyk, A. W., Richardson, C. C. & van Oijen, A. M. Simultaneous single-molecule measurements of phage T7 replisome composition and function reveal the mechanism of polymerase exchange. *Proc. Natl Acad. Sci. USA* **108,** 3584–3589 (2011).

45. MacMillan, A. M., Chen, L. & Verdine, G. L. Synthesis of an oligonucleotide suicide substrate for DNA methyltransferases. *J. Org. Chem.* **57,** 2989–2991 (1992).

46. Tanner, N. A. & van Oijen, A. M. in *Single Molecule Tools, Part B:Super-Resolution, Particle Tracking, Multiparameter, and Force Based Methods* (ed. Walter, N. G.) 259–278 (Academic, 2010).